Improving Accuracy of Quantitative Susceptibility Mapping Using Edge-Weighted L1 Regularisation

Meng-Chi Hsieh[1,2], Chung-Ming Chen[3], Kun-Hsien Chou[4], Ai-Ling Hsu[1,2], Ching-Po Lin[4], and Jyh-Horng Chen[1,2]

[1]*Graduate Institute of Biomedical Electronics and Bioinformatics, National Taiwan University, Taipei, Taiwan,* [2]*Interdisciplinary MRI/MRS Laboratory, Department of Electrical Engineering, National Taiwan University, Taipei, Taiwan,* [3]*Institute of Biomedical Engineering, National Taiwan University, Taipei, Taiwan,* [4]*Brain Connectivity Lab, Institute of Neuroscience, National Yang-Ming University, Taipei, Taiwan*

Target Audience: Researchers and clinicians interested in susceptibility MR mapping and tissue characterization for personalized medicine.

Purpose: Recently, Quantitative Susceptibility Mapping (QSM) widely shows its capability to quantitatively assess tissue composition. However, calculating susceptibility maps from phase images is an ill-conditioned problem, resulting in streaking artefact. To obtain artefact-free susceptibility map, several L1-based regularisations have been suggested. Nevertheless, conventional L1 method might run into under-estimation while the weighting of regularised term was raised for noise reduction. Herein, we proposed a novel approach, Edge-Weighted L1 (EW-L1), by improving L1 regularisation for more accurate estimation and less artefact in quantitative susceptibility map.

Theory: Our proposed method EW-L1, based on L1, involves the minimization of $\{\|b - F^{-1}DF\chi\|_2^2 + \lambda \cdot W \cdot \|G\chi\|_1\}$, where b is the internal field map, F is the three dimensions (3D) fast Fourier transform, χ is the susceptibility map, $D(k) = 1/3 - k_z^2/k^2$ is the transfer function of dipole, G is 3D gradient operator, λ is the Lagrange multiplier, and W *is the binary edge-weighting matrix*. For comparison, conventional L1 method was used by minimizing $\{\|b - F^{-1}DF\chi\|_2^2 + \lambda \cdot \|G\chi\|_1\}$ [1] with no modification factor W.

Methods: *Data acquisition and pre-processing:* Whole-head 3D GRE data were acquired at 3T MRI (Siemens, Erlangen, Germany) with imaging parameters: $FOV = 256 \times 224 \times 88$ mm^3, $voxel\ size = 1 \times 1 \times 2$ mm^3, TR/TE=27/20 ms, and flip angle=15 degree. MR images from individual element of coil array (12-channel) were combined and separated into magnitude and phase. Aliasing phase was resolved with 3D path-based unwrapping method [2], and the background field was estimated and removed by PDF [3]. The edge-weighting distribution W was the binary image derived from internal field map by gradient thresholding.

Numerical simulation: A 3D Shepp-Logan phantom (matrix=192^3 and FOV=20^3 cm^3) consisting of five susceptibility values (0.1, 0.2, 0.3, 0.4, and 0.5 ppm) was generated. Field map was calculated using Fourier relationship [4] and then added with zero-mean Gaussian noise (standard deviation=0.005 ppm). The edge-weighting distribution W was the binary image derived from ideal phantom (edges were set to zeros, and others were ones).

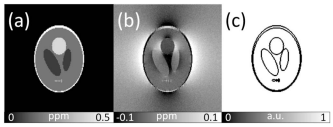

Fig. 1. (a) Numerical phantom with susceptibility. (b) Calculated field map (SNR=20). (c) Binary edge-weighting image.

Data processing: The steepest decent method [5] was employed with 30 and 100 iterations using both methods for *in vivo* and numerical data, respectively.

Analysis: For numerical simulation, the Root-Mean-Squared-Error (RMSE) was used as a metric to quantify the error obtained from either case. Moreover, accuracy in various λ was assessed by observing the slope of linear regression of ideal values versus estimated susceptibility. For *in vivo* data, estimated susceptibility values of several specific regions including Globus Pallidus (GP), Putamen (PU), Red Nucleus (RN), Substantia Nigra (SN), and Dentate Nucleus (DN) were quantitatively measured. The susceptibility difference between L1 and EW-L1 was assessed by t-test with significance determined at $p = 0.01$.

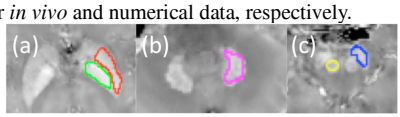

Fig. 2. ROI selections. (a) PU (red) and GP (green). (b) DN (pink). (c) SN (blue) and RN (yellow).

Results and Discussions: Fig. 3(a) compares the estimated susceptibility maps for numerical phantom using L1 and EW-L1 methods at $\lambda = 10^{-1.3}$. It is seen that the streaking artefact could be effectively eliminated by EW-L1. Furthermore, the EW-L1 method could preserve more edge details and prevent over smoothing while using larger λ. The RMSE were 0.0124 and 0.004 of using L1 and EW-L1, respectively. It indicates that the better resulting susceptibility map using EW-L1 could be achieved. Fig. 3(b) shows the slopes of the two methods at various λ. It demonstrates that, compared to L1, EW-L1 could provide highly accurate and stable estimation while rising λ for noise elimination. in Fig. 4, we compares the resulting susceptibility maps of *in vivo* brain by L1 and EW-L1 at $\lambda = 10^{-1.3}$. The susceptibility map by EW-L1 could preserve more edge details and avoid underestimation for using larger λ. The estimated susceptibility values by both methods were quantitatively assessed from five ROIs as shown in Fig. 5. In general, most of the calculated susceptibility values by EW-L1 were significantly higher than that by L1 ($p<0.01$). In combination of Results in Fig. 3, it suggests that the EW-L1 could provide more accurate assessment at larger λ.

Conclusions: We presented a novel EW-L1 method for accurate estimation of QSM. It has been shown through numerical simulation and human brain experiment that EW-L1 leads to susceptibility maps with suppressed artefact and more accurate measurements. Further validation is required for the *in vivo* brain study in the future

References: [1] Rudin et al., Physica D (1992). [2] Abdul-Rahamn et al., Applied Optics (2007). [3] Liu et al., NMR in Biomedicine (2011). [4] Salomir et al., Concepts in Magnetic Resonance Part B: Magnetic Resonance Engineering (2003). [5] Nocedal and Wright, Numerical Optimization (2006).

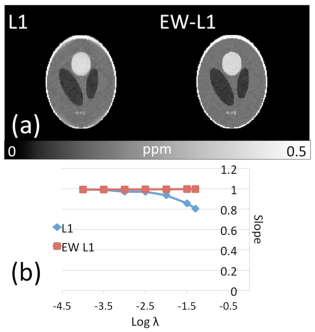

Fig. 3. (a) Comparison of estimated susceptibility by the two methods at $\lambda = 10^{-1.3}$ in numerical phantom. (b) The slopes of ideal value versus estimated susceptibility values using L1 and EW-L1 in various λ, respectively.

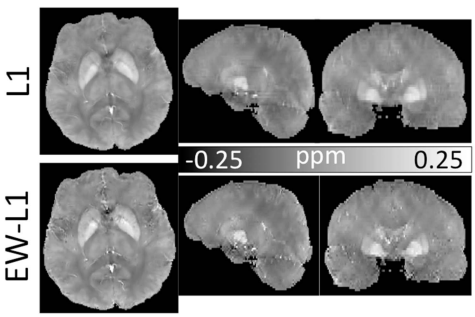

Fig. 4. Comparison of estimated susceptibility of a axial, a sagittal, and a coronal transection of human brain from single healthy subject using L1 (top row) and EW-L1 (bottom row) at $\lambda = 10^{-1.3}$. Compared to L1, using EW-L1 to calculate susceptibility map could preserve more edge details and avoid underestimation.

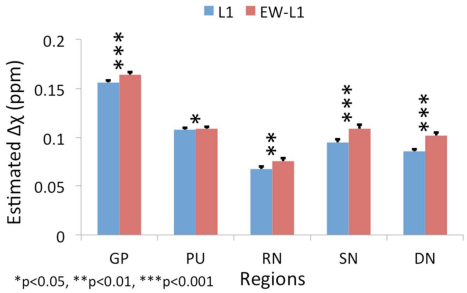

Fig. 5. Mean and S.E.M. (standard error of mean) of susceptibility values in ppm computed by the two methods for each ROI from single subject. It indicates that estimated susceptibility values by EW-L1 were significantly higher in GP, RN, SN, and DN ($p<0.01$).